JOINT INSTITUTE FOR NUCLEAR RESEARCH
Dzhelepov Laboratory of Nuclear Problems

FINAL REPORT ON THE START PROGRAMME

Development of the Monte Carlo model of the LED calibration system for the TAO detector

Supervisor:
Ph.D. Gromov Maxim Borisovich

Student:
Rudakov Peter, Russia
Lomonosov Moscow State University,
Faculty of Physics

Participation period:
July 10 - August 19,
Summer Session 2023

Dubna, 2023

Contents

1

Abstract

The research includes the development of a Monte Carlo model of the TAO detector LED (optical) calibration system by means of the Geant4 simulation toolkit and the SNiPER framework. The aim was to obtain a qualitative and quantitative assessment of the shadow area on the surface of the TAO Central Detector from the weight of the light source of the LED calibration system. An optical photon generator and models of the optical calibration system elements were developed as plug-ins of the TAO simulation package. An interface for controlling the input parameters of the simulation was also designed and implemented.

A simulation of the operation of the optical calibration system in various configurations was performed. The analysis of the simulation output data was carried out using a ROOT framework and the Python programming language. The dependence of the number of hits on SiPMs was plotted as a 3D "heatmap" for different simulation parameters. Then a histogram of the relative difference in the average number of hits on a SiPM for all the layers with and without the weight was drawn and analyzed. The shadow effect has been found to be small and it will not spoil the planned calibrations.

Introduction

This work was done within participation in the JINR START program under the supervision of Ph.D. and research fellow of the Dzhelepov Laboratory of Nuclear Problems Maxim Gromov. The research was related to the JUNO-TAO experiment in which the Dzhelepov Laboratory takes part actively. The goal was to perform a Monte Carlo simulation of the operation of the TAO detector LED calibration system. The following report describes the process of creating the light source model, the issues encountered throughout the development and ways to resolve them. Also, the document includes a description of the functionality of the current version of the model, the first simulation results and their preliminary analysis.

1 JUNO-TAO Experiment

The JUNO-TAO experiment consists of two detectors located at different distances from antineutrino sources. The main JUNO liquid scintillation detector (Jiangmen Underground Neutrino Observatory) is placed at the same distance of 52 km from two nuclear power plants, which serve as artificial sources of antineutrinos. The main purposes of creating the JUNO detector is to search for physics out of the Standard Model, to observe neutrino oscillations and to determine the neutrino mass hierarchy particularly. The JUNO detector is designed to achieve the maximum possible energy resolution and enough counting rate of events of inverse beta decay according to the coincidence scheme at the same time [1].

The Taishan Antineutrino Observatory (TAO) is a near detector located 30 m away from the reactor core. TAO was created in order to obtain a model-independent neutrino energy spectrum, which will let us perform a more accurate fitting of the experimental JUNO spectrum.

A liquid scintillator was also chosen to implement the TAO scientific program, the main photon detectors in the TAO detector are silicon photomultipliers (SiPM) in contrast JUNO where photomultiplier tubes (PMT) are used to register light from events in the sensitive area of the detector.

The Monte Carlo models of the JUNO and the TAO detectors have been created based on Geant4 [2] and the SNiPER framework (Software for Non-collader exPERiments) [3] to set up a virtual experiment. The model of the LED calibration system is implemented as a plug-in module of the general DetSim simulating package. The Monte Carlo model was developed using the object-oriented C++ and Python languages, and the analysis of the results was carried out using ROOT [4] and Python.

2 Development and implementation of the light source model

The TAO LED calibration system will be used to perform quantum efficiency test, SiPM gain check, imitation of real scintillation events, to test of the offline analysis pipeline and to provide extra reference information for spatial reconstruction.

The LED calibration system in the TAO detector consists of two LED sources with

wavelengths of 265 nm and 420 nm, the waveguide made of fiber, the quartz diffuser with the weight at the end of the fiber and the mechanical input system to control position in the detector within the automatic calibration unit (ACU) which principal scheme you can see in Figure 1. It is worth noting that the ACU fully automates the procedure of placing all sources into the sensitive area of the detector. The ACU is described in more detail in the article [5].
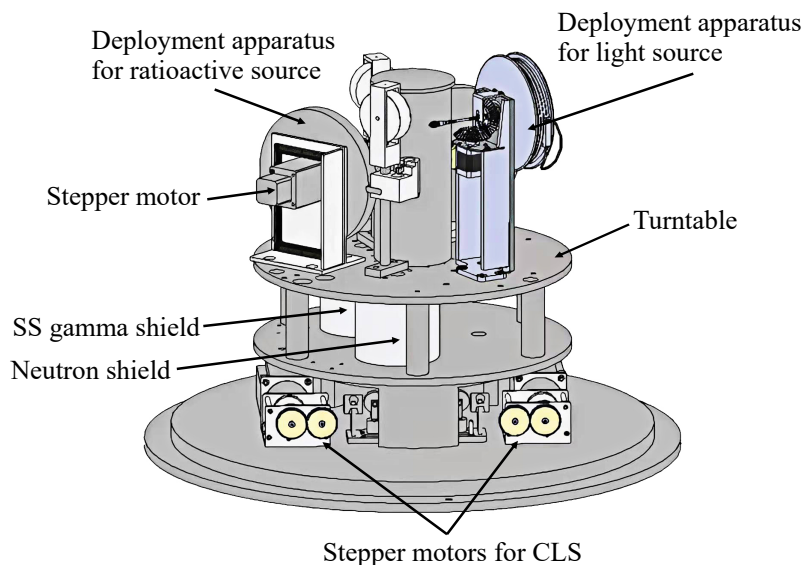

Figure 1: An overview of the Automated Calibration System.

The LED calibration system model (hereinafter referred to as optical calibration system — OCS) is designed to work out real calibration procedures using the LED system and to improve these procedures and to analyze the calibration data. In particular, to assess the presence of a shadow qualitatively and quantitatively, which presumably arises due to the shielding of a part of the inner surface of the spherical Central Detector with a metalic weight.

The development of the OCS Monte Carlo model as a module of the existing simulation program has its own specifics. The following stages of the work can be distinguished:

- Implementation of the light pulse generator as SNiPER GenTool.

- Optimization of the simulation code to achieve acceptable resource intensity and performance.

- Adding OCS model.

- Modification of the simulation data output procedure in order to ensure the possibility of extracting the information of interest during subsequent analysis in the most convenient way.

- Performing the simulation of the calibration with the light source.

- Output .root files analysis and weight shadow evaluating.

4

2.1 Using the SNiPER framework

The JUNO-TAO collaboration uses the SNiPER framework [6] to automate the transfer of virtual experiment data to the subsequent stages of data processing, to coordinate data types and to simplify the work with them of a large number of diverse specialists. This allows us to perform flexible modeling, to control program modules in runtime, due to SNiPER presence at all stages of modeling and data processing. The structure of the SNiPER classes can be seen in Figure 2.
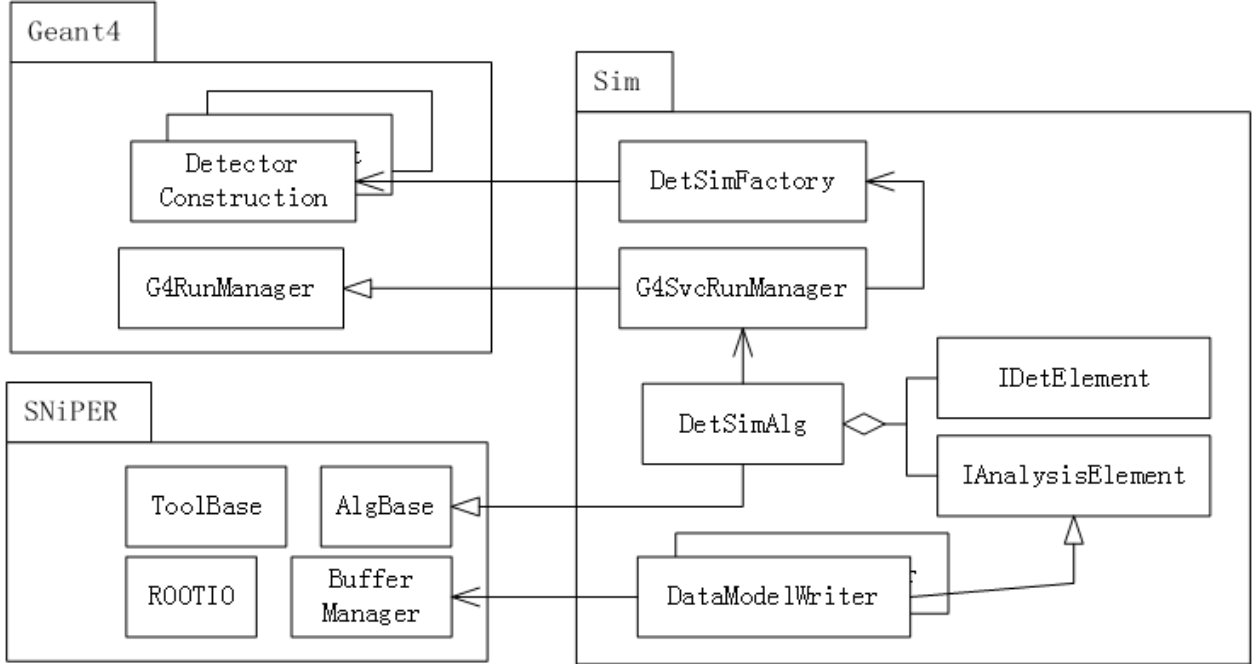

Figure 2: Simulation framework design.

The work was started by the implementation of the OptGunGenTool particle generator, capable of launching the primary optical photons of the corresponding energy both isotropically and into an oriented cone. This is the GenTool child class created according to the logic of the framework, which provides to fulfill reading of generator startup parameters from the console[1] along with other SNiPER classes [3].

This approach in development allows us to create a flexible simulation tool that can be controlled without recompiling the entire project. an independent non-trivial task. The presence of the framework in the project without the full-fledged documentation led to the separation of correct framework infrastructure development into a complex goal.

2.2 LED calibration system simulation module based on Geant4

Despite the complexity of using the SNiPER framework, the main task was to create an adequate model based on the Geant4 software package [2]. Initially, the development of an optical flash generator designed to simulate the LED source was carried out by modifying

---

[1]At this stage of development of the project .mac files are not used to set startup parameters.

the universal GunGenTool generator, but over time, changes accumulated and this required the development of the generator to be placed in a separate OptGunGenTool class and writing documentation for this module on the internal collaboration Wiki. In addition, it was necessary to modify the geometry in the TaoDetectorConstruction class in order to create a plug-in part corresponding to the diffuser and the weight of the LED calibration system. Also, in order to reduce the output of technical information during simulation and save resources, the logging detail was lowered by making changes to a number of the DetSim classes. Information about photons detected by SiPMs was added to the data model of the simulation system. For each particle, its coordinates and the identifier of the SiPM into which it hitted are stored.

2.3 Development of the OptGunGenTool generator class

At the moment, the OptGunGenTool generator allows:

- To set the position of the source.

- To launch a large ($> 10^6$) number of photons in one event.

- To create monoenergetic optical photons with an arbitrary direction of the particle.

- To create photons whose momentum is oriented inside a cone with a given apex angle.

- To orient in space the area into which the photons are launching (cone).

The following parameters are fully controlled:

1. The number of photons in the flash.

2. Position of the source (diffuser).

3. Mode of operation of the generator (isotropic generation or cone generation).

4. Orientation and apex angle of the cone.

2.3.1 Implementation of random pulse generation in a cone and its orientation in space

When developing a method of the OptGunGenTool class that creates photon pulses randomly distributed inside a cone, the problem of uniform points generation on a sphere was encountered. It's solution was implemented as follows:

1. The sample of azimuth angle cosines was generated according to a uniform distribution.

2. The sample of polar angles was generated according to a uniform distribution.

3. Two mutually orthogonal unit vectors $\mathbf{e_1}$, $\mathbf{e_2}$ were set using the methods of vector algebra. Both of them are orthogonal to the given axis $\mathbf{e_3}$ of the cone, where $|\mathbf{e_3}| = 1$. The random unit vector within the cone will be a vector x of the form

$$\mathbf{x} = \cos\theta(\cos\phi\mathbf{e_1} + \sin\phi\mathbf{e_2}) + \cos\theta\mathbf{e_3} \tag{1}$$

where ϕ is an polar angle, θ is an azimutal angle laying in $[0, \theta_0]$ and θ_0 is a half of cone apex angle.

Next, the rotation of the cone is carried out by rotating the basis vectors $\mathbf{e_1}$, $\mathbf{e_2}$ and $\mathbf{e_3}$ by a simplified rotation matrix[2] composed of Euler angles.

2.3.2 Performance issues and their solutions

Logging

In the initial version, the simulation program conducts double logging of all processes (two output streams namely SNiPERLog and G4cout are created) and prints out reference information for each vertex for the first ten events, which increases the size of the logs of the optical light pulse generator to unacceptable values about 1 GB, in case of one million primary particles in one event.

Lowering the logging level were mainly performed by standard Geant4 and SNiPER tools. However, there was the DetSim simulation package output of some debugging messages to the standard cout stream in the code, which required searches and manually commenting out of the output in several classes inheriting Geant4 base classes. At the moment, these explicit changes are documented and stored in the rudakov_optical_calibration_system_taosw branch of the TAOSW git repository.

Measures to reduce the simulation logs allowed us to achieve an output file size of about 130 KB or 2100 lines in case of 100 events for a million primary photons in each event. The performance has been improved several times: to simulate 10 events of 100 thousand photons each time was reduced from 12 to 3 minutes of real time.

Saving tracks of the original particles

In the TaoAnalysisManager class, the tracks of all the original particles were saved, which led to fails when trying to launch more than 100 thousand source photons in one event. The most likely cause of the failure is a lack of RAM, so it was decided to implement an interface to optionally disable this functionality.

Disabling the saving of the original particle tracks does not lead to loss of useful information, since it does not affect the SiPM photon detection data, and individual photon tracks are of no value for solving OCS-related problems. Moreover, the limit on the number of primary photons of 100 thousand in one flash was lifted and successful runs were carried out with up to several million photons in one event.

The performance can be improved many times, for example, for 10 events of 100 thousand primary photons each time was reduced from 3 minutes to 0.7 minutes of real time. The final execution time to create a sample with satisfactory size of 100 events of 1 million primary photons each was about 70-80 minutes of real time.

---

[2]The intrinsic rotation angle does not matter due to the axial symmetry of the cone.

2.4 Models of the diffuser and weight

Figure 3: The drawing of the diffuser and the weight. All dimensions are in mm.

At the moment, a simplified model of the diffuser and the weight is implemented, namely, the weight is represented as a cylinder made of invar, with an inner channel along the axis and the diffuser is a quartz solid sphere. The weight is away from the diffuser sphere surface at a distance of 25.5 mm, this allows us to expect the small weight shadow size due to the smallness of the angle at which the weight is visible from the scintillation photon birth region. The linear dimensions were set according to Figure 3. The optical properties of the diffuser and the weight surface material shown in Table 1 are set. Also, the diffuser–scintillator and the weight–scintillator boundaries are set.

Table 1: Material properties in the model.

Material	Enegry, eV	Refraction index	Absorption lenght, mm	Reflection coefficient	Transmission efficiency
quartz	2.50–3.50	1.47	70–58	–	–
	3.60–3.90	1.48	58–56	–	–
	4.0–4.74	1.49	55–10	–	–
invar	2.50–4.74	–	–	0.4	0

A corresponding flag has been added to control the light source geometry. It is possible to apply only the diffuser, only the weight, the diffuser and the weight together or not to apply the models of the LED calibration system elements at all.

There were made blanks for the further implementation of the quartz tube between diffuser sphere and the weight, the channel for the fiber and for the glue filling the channel and attaching the fiber to the rest of the light source elements.

2.5   Interface for setting input parameters

A command-line interface was developed to control the input parameters of the OCS simulation. There is a detailed description of this interface that provides access to variables for modification in Table 2.

3   Model testing and results analysis

The simulations the description of which is given in Table 3 were carried out under various conditions to assess the influence of the diffuser model.

Table 3: Configurations of the simulation runs.

N	Energy, eV	Wavelength, nm	Cone apex angle, deg.	Geometry	Figure
1	3	413	360	without OCS geometry	4
2	3	413	24	only weight	5
3	4.7	264	360	without OCS geometry	6
4	4.7	264	24	only weight	7
5	4.7	264	24	only weight, invar reflection index is reduced to 0.01	8
6	4.7	264	24	only diffuser	9
7	4.7	264	24	with diffuser and weight	10

Statistics for any configuration of the virtual experiment in the amount of 100 events for 1 million primary particles in each event were collected.

Table 2: Description of the added input parameters and the respective flags for the command-line interface.

Flag	Usage	Variable	In file
--flash	to specify the number of photons in a single flash	int m_numberOfPhotons	OptGunGenTool
--cone-axis-azimutal-angle	to specify the azimuthal rotation angle of the axis of the cone into which the primary photons are directed (degrees)	double m_coneAxisAzimutalAngle	
--cone-axis-polar-angle	to specify the polar rotation angle of the axis of the cone into which the primary photons are directed (degrees)	double m_coneAxisPolarAngle	
--cone-apex-angle	to specify the cone apex angle (degrees)	double m_coneApexAngle	
--momentums	to specify the array of energies of photons, should be specified by one energy	std::vector<double> m_particleMomentums	
--momentums-interp	to specify the momentum interpretation, at the moment, the generator only supports the default value 'kinetic energy'	std::string m_momOrKEOrTE	
--momentums-mode	to specify the distribution type, specify 'Cone' after a flag to choose cone distribution instead of uniform generation by default	std::string m_particleMomentumMode	
--nonePrimPartTracks	put this flag if you want to disable saving primary particles tracks, it is necessary to use it if you are going to run more than 10^6 of photons	bool m_nonePrimPartTracks	TaoAnalysisManager
--enableDiffuser	put this flag if you are going to enable the diffuser	bool m_enableDiffuser	TaoSimFactorySvc
--enableWeight	put this flag if you are going to enable the weight	bool m_enableWeight	

The photon energy of 3 eV corresponds to blue visible light with a wavelength of about 413 nm, and 4.7 eV corresponds to ultraviolet light with a wavelength of 264 nm. Ultraviolet is rapidly absorbed by the scintillator substance and is re-emitted with a wavelength shift in a random direction. The design of the diffuser provides that ultraviolet photons reach the scintillator in some finite area on the quartz sphere surface, which ensures satisfactory isotropy of the source radiation [5]. In addition, the weight is at a distance of 25.5 mm from the diffuser sphere surface. This allows us to expect the small size of the shadow created by the weight due to the smallness of the angle at which the weight is visible from the scintillation photon origin volume.

Testing the model in modes with a photon energy of 3 eV made it possible to control the correctness of the generator functionality implementation.

In all tests, the cone axis is oriented towards the negative direction of the Z axis.

Simulation in configuration 1 shows that there is almost isotropic light pulses generation in a cone mode with cone apex angle equal to 360° as you can see in Figure 4. However, we still have about 10 % number of hits on SiPM fluctuations between minimum and maximum value over the CD sphere.

The test in the configuration 2 gives the result corresponding to the expected: blue visible light freely passes through the transparent scintillator substance and reaches SiPM's as you can see in Figure 5.

The next test 3 demonstrates isotropic generation of 4.7 eV photons with disabled light source elements model. There is an almost ideal isotropy of hits on SiPMs due to the re-emission of photons in the scintillator substance as you can see in Figure 6. This result corresponds to the expected one for these input parameters. Therefore, there are a quite big for this size of statistics 5 % fluctuations of hits on SiPMs over the CD sphere. Possible reasons for this effect are the imperfection of the currently used pseudorandom number generator and the issues of the random light pulses generating procedure.

The test in configuration 4 makes it possible to make a qualitative assessment of the weight enabling effects. There is a shadow area in the upper row of SiPMs in the northern hemisphere of the Central Detector and the illumination of the lower row of SiPMs in the southern one as you can see in Figure 7. The presence of the shadow area is explained by shielding part of the Central Detector surface with the weight. Regarding the illumination of the lower layer, there was an assumption that it is caused by reflected light from the weight. The following test confirmed this hypothesis.

The simulation in configuration 5 was performed with the invar reflection coefficient reduced to 0.01. You can see the lack of illumination in Figure 8. The value from Table 1 was restored for subsequent simulations.

You can see the simulation results in configuration 6 on a 3D heatmap graph showing the number of SiPM hits in Figure 9. The lower hemisphere is slightly better illuminated than the upper one, which can be seen by the color change on the corresponding projections of the sphere. It can be explained by absorption in a quartz diffuser. Integral estimation of the number of SiPM hits in the upper and lower hemispheres allowed us to estimate the magnitude of this effect. The relative difference in the illumination of the hemispheres was 1.7 %.

The simulation results in configuration 7 can be seen on a similar graph in Figure 10. The results showed the presence of increased illumination areas of SiPMs in the lower hemisphere
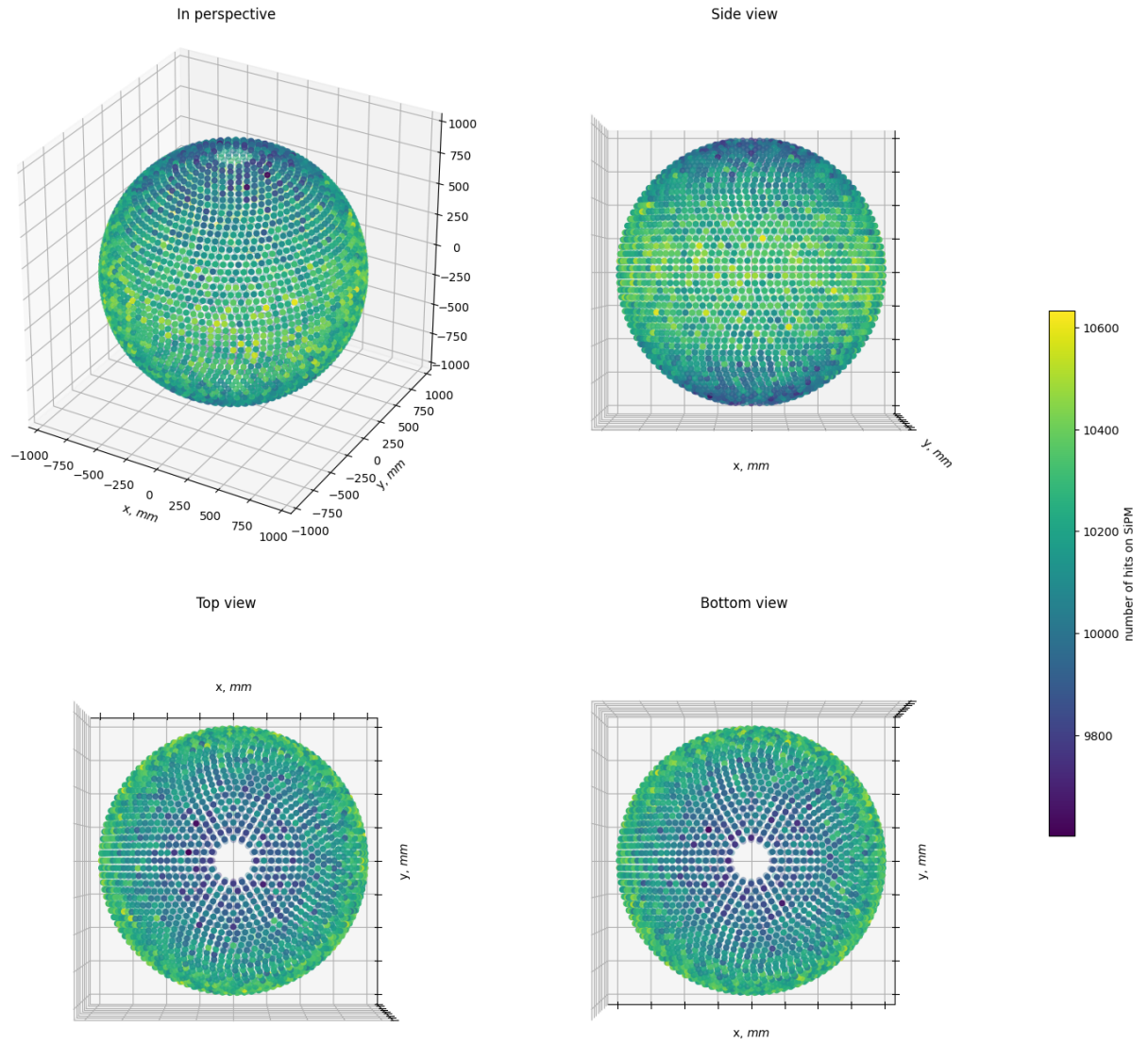
Figure 4: The number of hits on SiPMs. The generator is in the cone mode with energy of photons of 3 eV and the cone apex angle of 360°. The diffuser and the weight are disabled.

In perspective

Side view

Top view

Bottom view
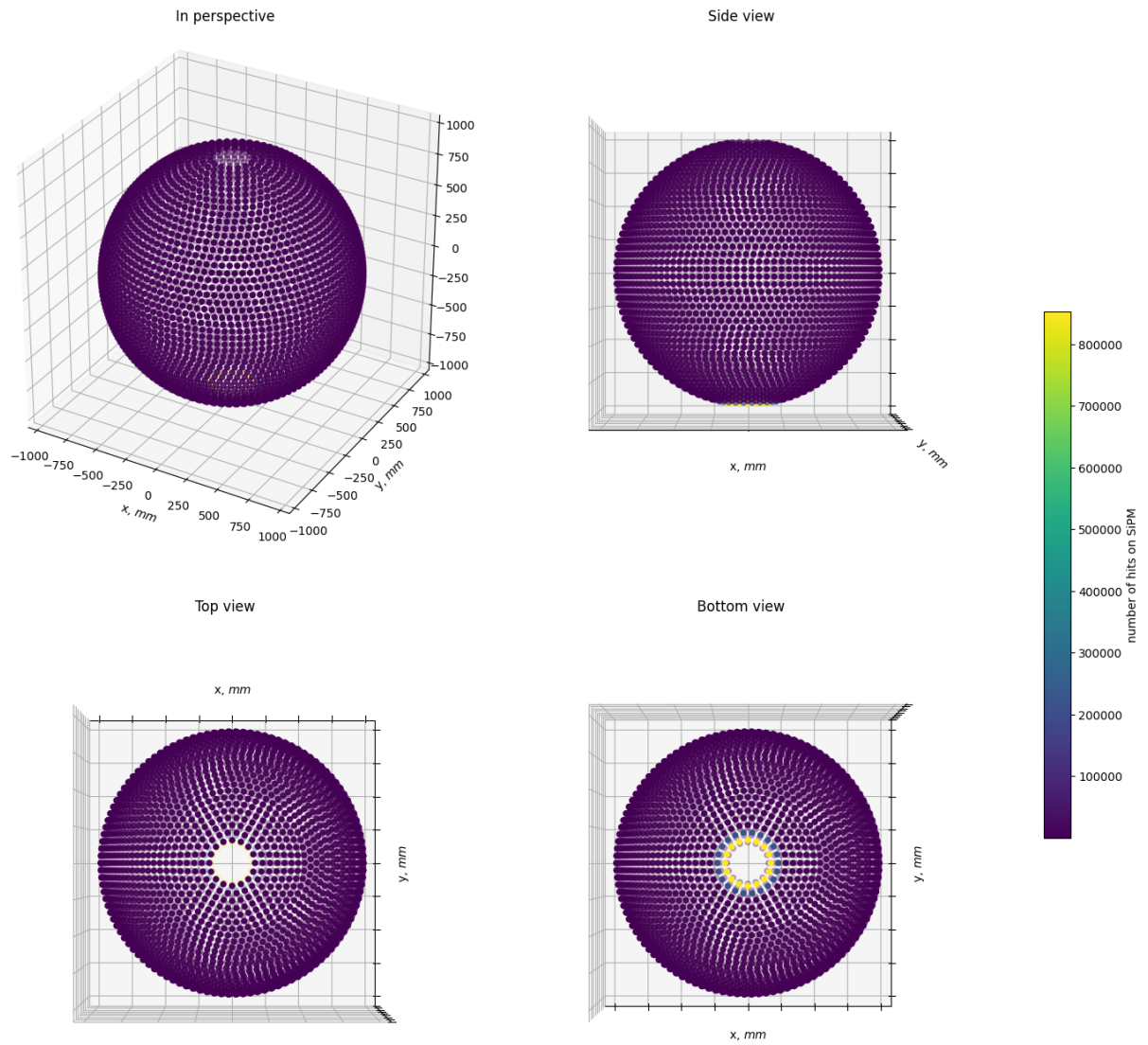
Figure 5: The number of hits on SiPMs. The generator is in the cone mode with energy of photons of 3 eV and the cone apex angle of 24°. The weight is enabled.
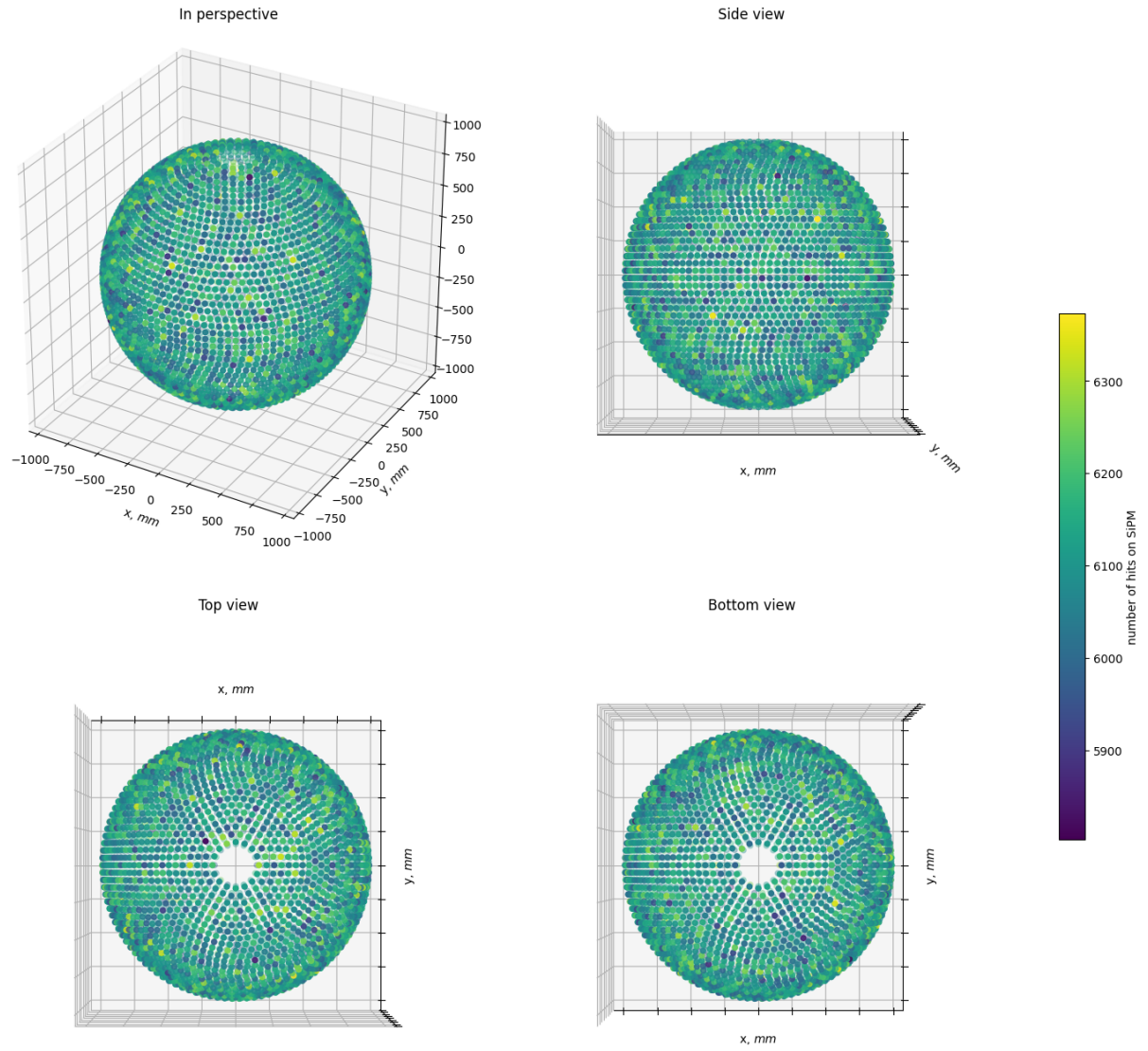
Figure 6: The number of hits on SiPMs. The generator is in the cone mode with energy of photons of 4.7 eV and the cone apex angle of 360°. The diffuser and the weight are disabled.
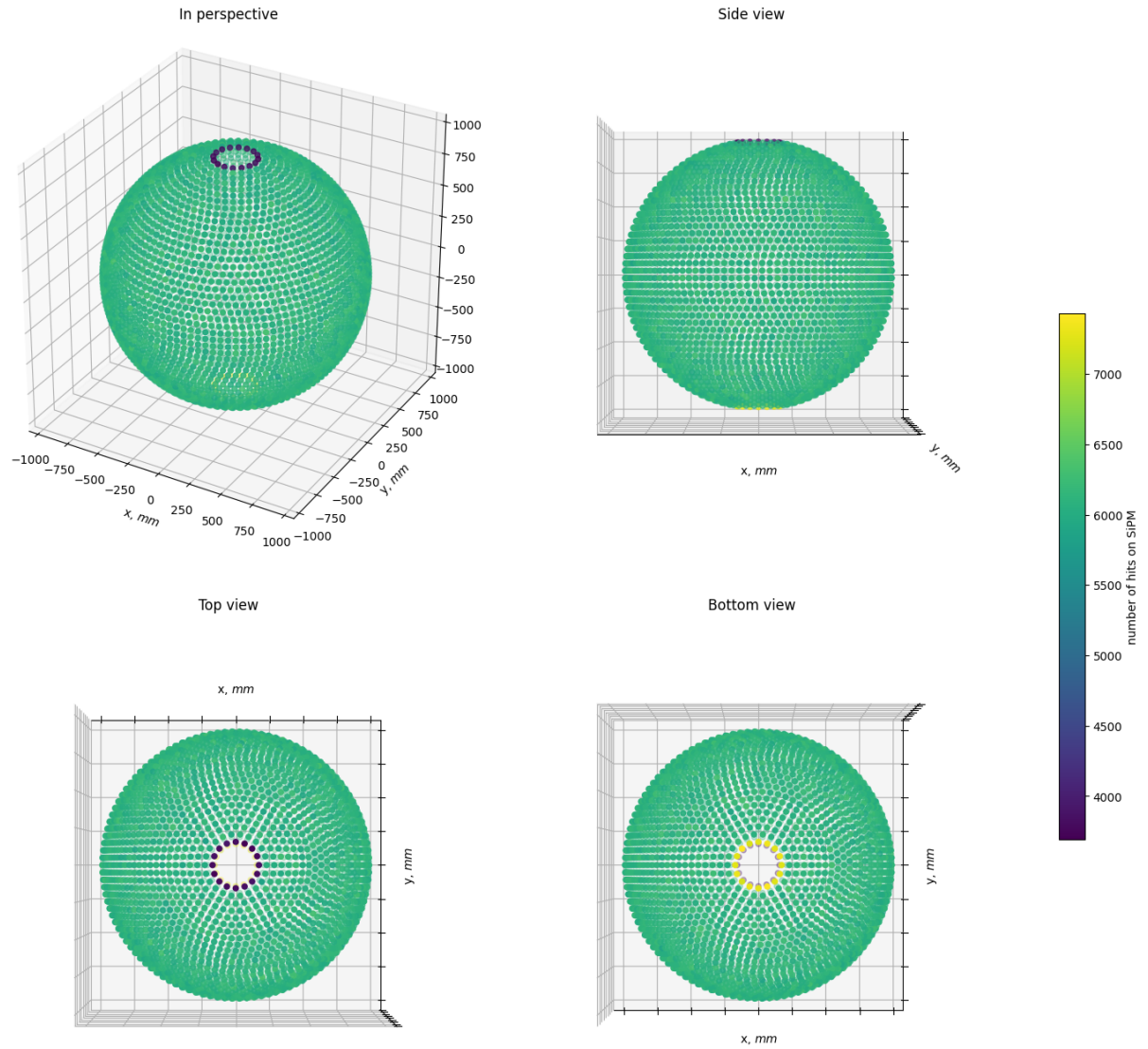
Figure 7: The number of hits on SiPMs. The generator is in the cone mode with energy of photons of 4.7 eV and the cone apex angle of 24°. The weight is enabled.

15

Figure 8: The number of hits on SiPMs. The generator is in the cone mode with energy of photons of 4.7 eV and the cone apex angle of 24°. The weight is enabled. The invar reflection index is reduced to 0.01.
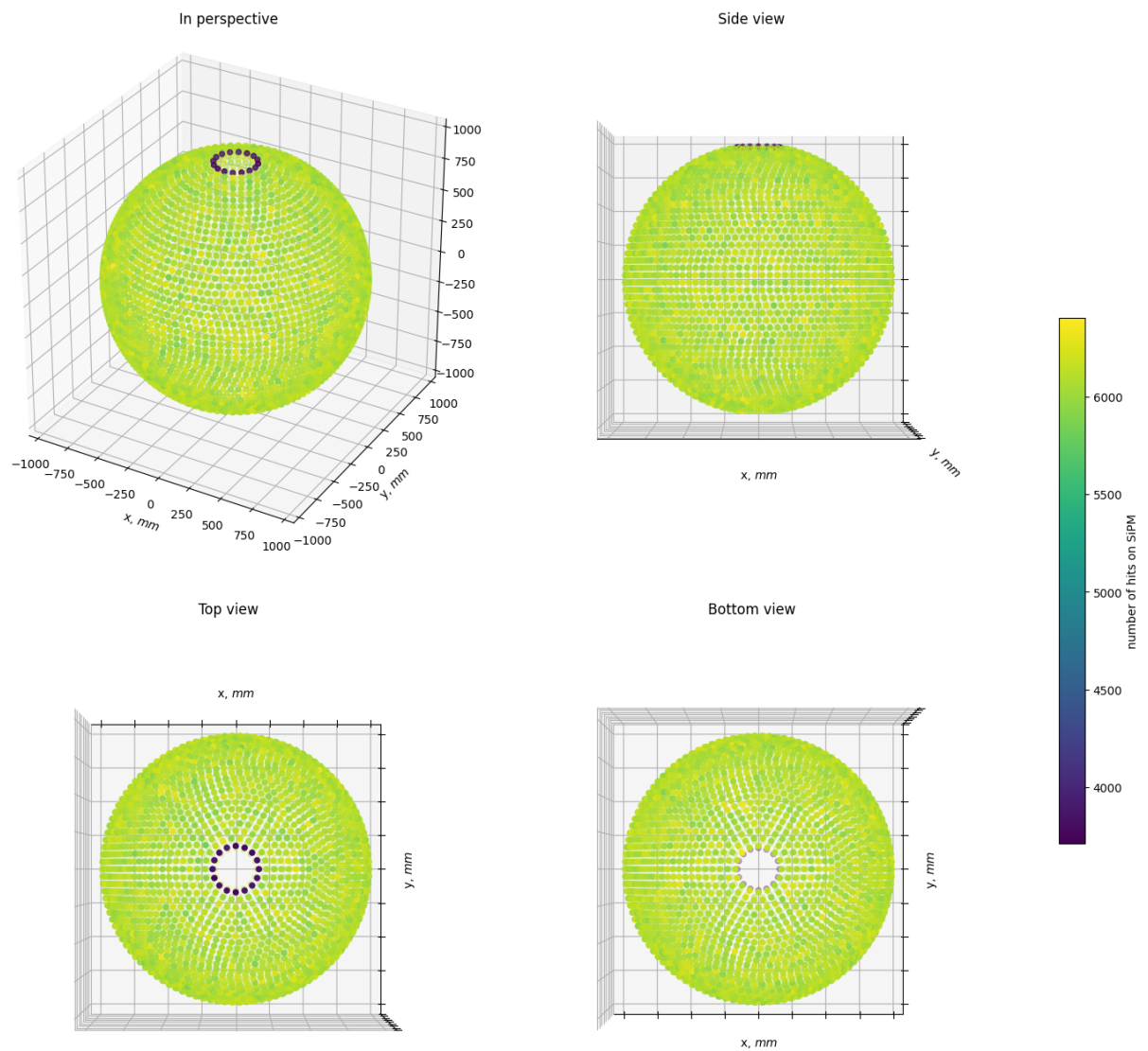
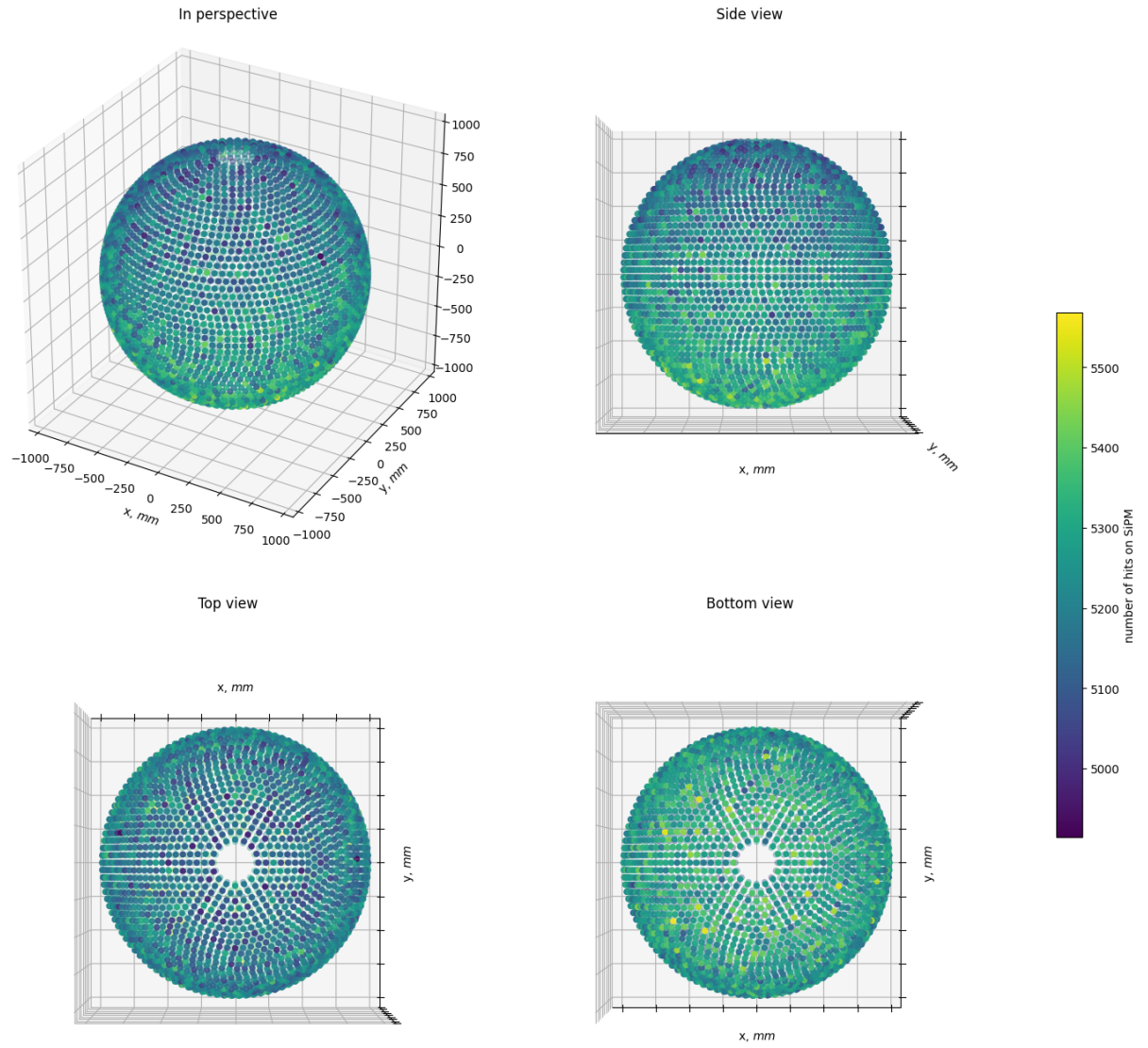Figure 9: The number of hits on SiPMs. The generator is in the cone mode with energy of photons of 4.7 eV and the cone apex angle of 24°. The diffuser is enabled.

17

and reduced illumination in the upper one (shadow). Namely, the layers of SiPMs are clearly distinguished near the poles of the sphere with a sharply different number of hits. The effect of different illumination of the upper and lower hemispheres of the Central Detector due to absorption in the diffuser substance is also noticeable on this 3D heatmap.
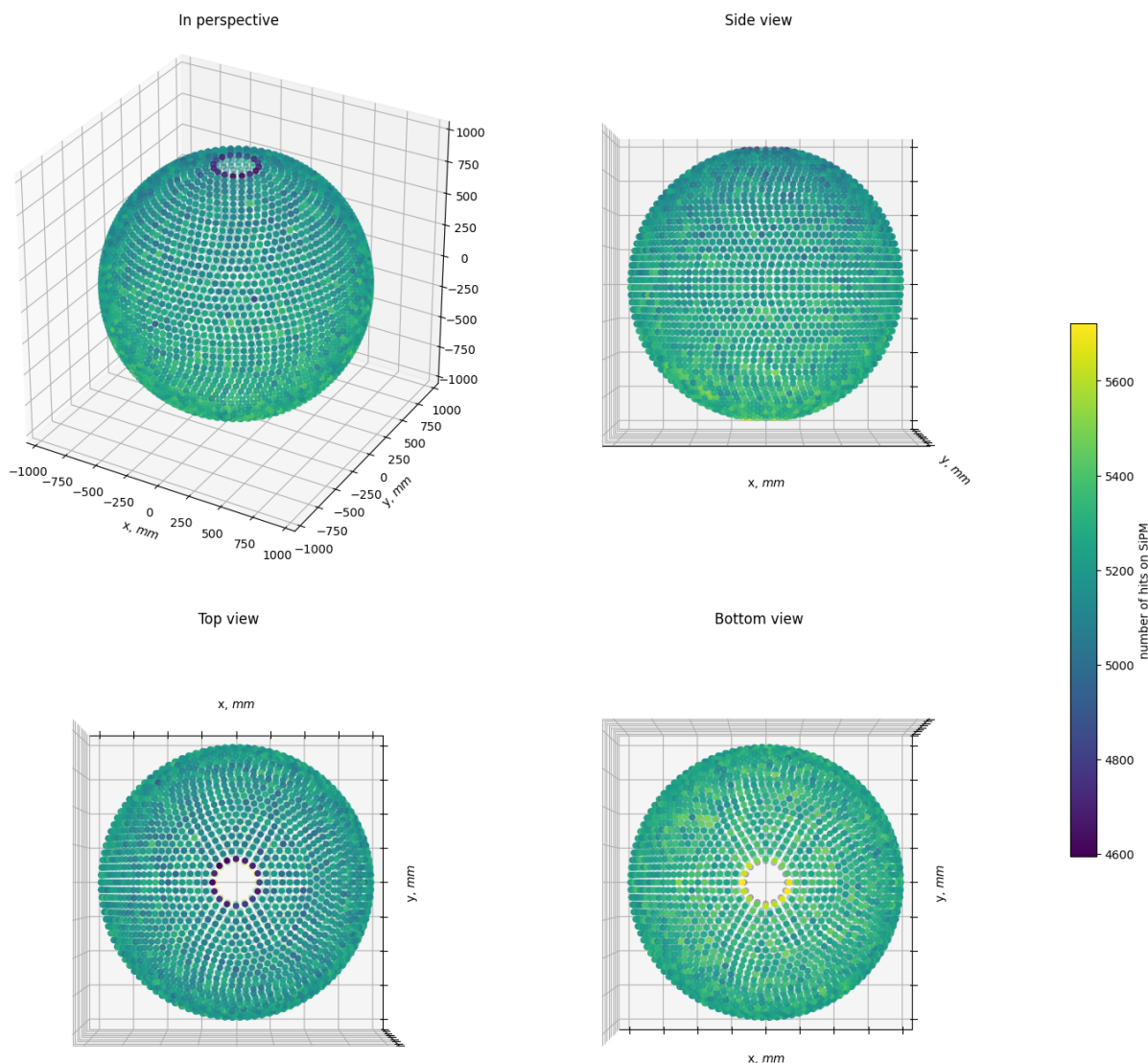

Figure 10: The number of hits on SiPM. The generator is in the cone mode with energy of photons of 4.7 eV and the cone apex angle of 24°. The diffuser and the weight are enabled.

A quantitative assessment of the shadow and illumination was performed by subtracting the results on the numbers of hits on individual SiPMs in the configuration without weight from the number of received hits with the enabled weight. The estimate of the shadow created by the weight and obtained in this way was integrated along the polar angle within each horizontal SiPM layer and then normalized by the number of SiPM in this layer. The

relative SiPM hits difference expressed as a percentage of the average value (hits), depending on the azimuth angle of the SiPM layer (measured from the positive direction of the Z axis) is shown in the histogram in Figure 11.

This graph shows a significant decrease in the illumination for only the extreme SiPM layer near the north pole and allows us to quantify this drop, which will be taken into account in the future when calibrating the TAO detector. Also, the illumination is limited and well localized in the SiPMs boundary layer at the south pole.
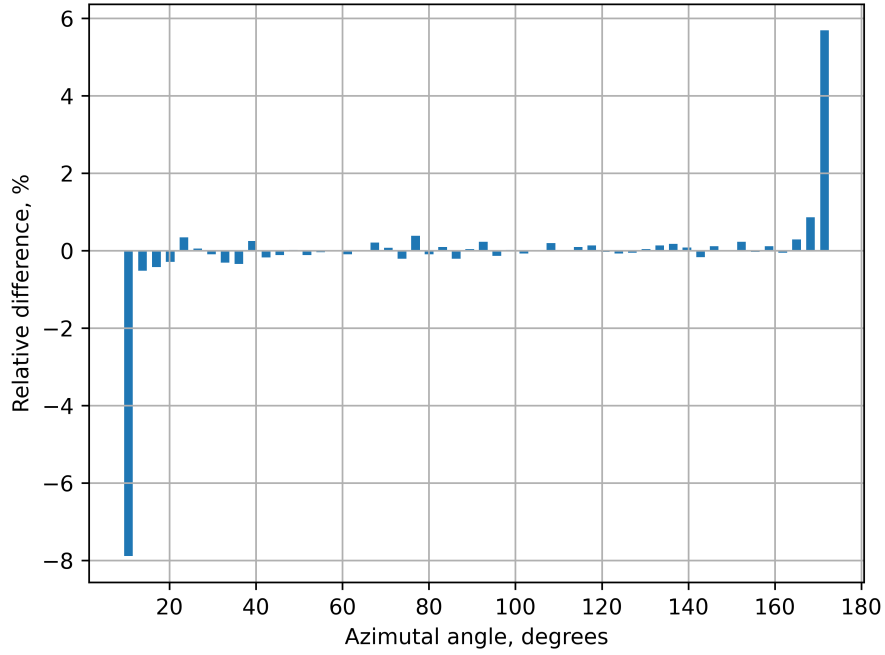

Figure 11: The relative difference of hits on SiPM by layer between simulations in configurations 5 and 6.

Conclusion

During the development of the LED calibration system model the features of the TAOSW software package and its DetSim module were taken into account. Particularly, the model is integrated into the SNiPER framework and architecturally implemented as a plug-in package for simulation.

When creating the model the problems of generating random light pulses directed into a cone according to a uniform distribution and the problem of turning the cone were solved. Also, all performance problems that arose during the work on the model were solved, in particular, the size of logs were successfully reduced and the ability to disable saving tracks of the original particles was implemented.

The results obtained for blue light photons with a wavelength of 413 nm and the respective energy of 3 eV correspond to expectations. The light from the OCS source freely passes through the liquid scintillator medium transparent to it and to a greater extent reaches the SiPMs of the Central Detector inside the initial cone, an insignificant number of photons reaches the SiPMs outside the initial cone due to scattering in the scintillator substance.

The results for photons of ultraviolet light with a wavelength of 264 nm and the respective energy of 4.7 eV showed that the shadow from the weight in the presence of the diffuser covers only three rows of SiPMs near the north pole of the Central Detector and the decrease in the number of photons relative to the results without the weight is 8% for the extreme layer and is within 1% for the next two layers. The illumination in the lower hemisphere is approximately 6% for the lowest layer and 1% for the second one from the bottom chimney. The extra light around the south pole can be explained by the reflection of secondary photons from the weight.

The simulation results allowed us to confirm the OCS parameters satisfactory for the calibration tasks. In the course of this work, the foundation was laid for the creation of an improved LED calibration simulation system, which will include an augmented OCS elements models, the ability to change the position of the diffuser in the space of the TAO CD and will allow using the results obtained during the simulation at subsequent stages of data analysis.

References

1. *Djurcic Z. et al.* JUNO Conceptual Design Report. 2015. Aug. arXiv: 1508.07166 [physics.ins-det].

2. *Asai M.* Introduction to GEANT4 // CERN School of Computing (CSC 2000). 09/2000. P. 107–117.

3. *Zou J. H. et al.* SNiPER: an offline software framework for non-collider physics experiments // J. Phys. Conf. Ser. 2015. Vol. **664**, № 7. P. 072053.

4. ROOT — An object oriented data analysis framework // Nuclear Instruments Methods in Physics Research Section A-accelerators Spectrometers Detectors and Associated Equipment. 1997. Vol. **389**, № 389. P. 81–86.

5. *Xu H. et al.* Calibration strategy of the JUNO-TAO experiment // Eur. Phys. J. C. 2022. Vol. **82**, № 12. P. 1112. arXiv: 2204.03256 [physics.ins-det].

6. *Lin T. et al.* The Application of SNiPER to the JUNO Simulation // J. Phys. Conf. Ser. / ed. by *R. Mount, C. Tull*. 2017. Vol. **898**, № 4. P. 042029. arXiv: 1702.05275 [physics.ins-det].

Acknowledgements

I would like to express my gratitude to my scientific supervisor Maxim Gromov for a great time spent solving non-trivial problems and the experience of participating in the modern scientific research of an international team of scientists.

Separately, I want to express appreciation and thank the student from China Jiayang Xu for the clarifications regarding the principals of the TaoAnalysisManager work.

I also want to thank the staff of the Dzhelepov Laboratory for the exchange of experience, pleasant pastime and interesting conversations during tea parties.

And also many thanks to the organizers of the START Program for the opportunity to take part in scientific work together with the JINR team.

Appendix

Table 4: The complete table of the material properties in the model.

Material	Enegry, eV	Refraction index	Absorption lenght, mm	Reflection coefficient	Transmission efficiency
quartz	2.50	1.47	70	–	–
	2.60	1.47	69	–	–
	2.70	1.47	68	–	–
	2.80	1.47	66	–	–
	2.90	1.47	65	–	–
	3.0	1.47	62	–	–
	3.10	1.47	61	–	–
	3.20	1.47	60	–	–
	3.30	1.47	59	–	–
	3.40	1.47	58	–	–
	3.50	1.47	58	–	–
	3.60	1.48	58	–	–
	3.70	1.48	58	–	–
	3.80	1.48	57	–	–
	3.90	1.48	56	–	–
	4.0	1.49	55	–	–
	4.10	1.49	54	–	–
	4.20	1.49	55	–	–
	4.30	1.49	54	–	–

Table 4: The complete table of the material properties in the model. (Continued)

Material	Enegry, eV	Refraction index	Absorption lenght, mm	Reflection coefficient	Transmission efficiency
	4.40	1.49	54	–	–
	4.50	1.49	53	–	–
	4.60	1.49	53	–	–
	4.70	1.49	53	–	–
	4.74	1.49	10	–	–
invar	2.50	–	–	0.4	0
	2.60	–	–	0.4	0
	2.70	–	–	0.4	0
	2.80	–	–	0.4	0
	2.90	–	–	0.4	0
	3.0	–	–	0.4	0
	3.10	–	–	0.4	0
	3.20	–	–	0.4	0
	3.30	–	–	0.4	0
	3.40	–	–	0.4	0
	3.50	–	–	0.4	0
	3.60	–	–	0.4	0
	3.70	–	–	0.4	0
	3.80	–	–	0.4	0
	3.90	–	–	0.4	0
	4.0	–	–	0.4	0
	4.10	–	–	0.4	0
	4.20	–	–	0.4	0
	4.30	–	–	0.4	0
	4.40	–	–	0.4	0
	4.50	–	–	0.4	0
	4.60	–	–	0.4	0
	4.70	–	–	0.4	0
	4.74	–	–	0.4	0